Colloids and Surfaces B: Biointerfaces 253 (2025) 114727

Contents lists available at ScienceDirect

Colloids and Surfaces B: Biointerfaces

journal homepage: www.elsevier.com/locate/colsurfb

Impact of different chemical debridement agents on early cellular responses to titanium dental implants: A transcriptome-based *in vitro* study on peri-implant tissue regeneration

Qiang Wang [a], Håvard Jostein Haugen [a,*], Dirk Linke [b], Ståle Petter Lyngstadaas [a], Ólafur Eysteinn Sigurjónsson [c,d], Qianli Ma [a,**]

[a] Department of Biomaterial, Faculty of Dentistry, University of Oslo, Norway
[b] Department of Biosciences, Faculty of Natural Sciences, University of Oslo, Norway
[c] School of Science and Engineering, Reykjavík University, Reykjavík, Iceland
[d] The Blood Bank, Landspitali, The National University Hospital of Iceland, Reykjavík, Iceland

ARTICLE INFO

Keywords:
Titanium implant surface
Peri-implantitis
Cytocompatibility
Chemical cleaning devices

ABSTRACT

Background: Poor peri-implant health leads to biofilm accumulation, peri-implantitis, and bone loss. Chemical debridement may help maintain peri-implant health, but its effects on peri-implant cells remain unclear.
Methods: Five cleaning agents—hydrogen peroxide (H2O2), Poloxamer, H2O2 +Poloxamer, Perisolv, and Paroex—were applied on titanium (Ti) surfaces. Mouse pre-osteoblasts (MC3T3-E1), human gingival fibroblasts (HGF), and human bone marrow stromal cells (hBMSC) were cultured on agent-treated Ti surfaces for up to 120 minutes to assess morphology, cytotoxicity, adhesion, and proliferation. RNA sequencing was performed on hBMSC.
Results: Except for Poloxamer, all treatments inhibited cellular spreading. Paroex increased cytotoxicity and inhibited proliferation. Perisolv impaired hBMSC adhesion and variably affected proliferation. H2O2, alone or with Poloxamer, elevated cytotoxicity and inhibited adhesion in hBMSCs but not MC3T3-E1 or HGF. In contrast, Poloxamer-treated Ti surfaces enhanced adhesion and proliferation across all cell types. RNA sequencing revealed that oxidant-based treatments (H2O2, H2O2 +Poloxamer, Perisolv) suppressed key genes for proliferation (HMGA2, JAG1, NOTCH1, YAP1, TBX3), anti-apoptosis (MCL1, BCL2L2), and adhesion (ITGA2, ITGB3, SPP1), while inhibiting MAPK, PI3K-Akt, and pluripotency pathways.
Conclusion: Commercial agents like Perisolv and Paroex impair hBMSC function, with Paroex demonstrating significant cytotoxicity. H2O2 exhibits toxicity, particularly to hBMSCs. Poloxamer improves cell attachment and growth. Given these findings, careful selection of debridement agents is critical to balance cleaning efficacy and cytocompatibility. The adverse effects on hBMSCs necessitate prompt removal postapplication. Further research on biomaterials supporting tissue regeneration postdebridement is needed to restore peri-implant health.

1. Introduction

Each year, approximately 5.5 million dental implants are surgically placed in the United States, with an anticipated long-term failure rate ranging from 3 % to 10 % [1]. Titanium (Ti) is widely used as an implant material due to its excellent biocompatibility, favorable mechanical properties, and corrosion resistance [2]. However, patients exhibiting poor plaque control and not attending regular maintenance therapy can develop immune-mediated biological complications, which are attributed to peri-implant diseases, such as peri-mucositis and peri-implantitis [3]. Microbial residuals can impede healing and re-osseointegration by initiating inflammation, potentially leading to peri-implantitis-a condition involving soft tissue inflammation, bone loss, and significant clinical and economic consequences [4,5]. Thus, minimizing oral biofilm accumulation on implants is essential for reducing peri-implant inflammation, as the long-term success of dental implants heavily

* Correspondence to: Geitmyrsveien 71, Oslo 0455, Norway.
** Corresponding author.
E-mail addresses: qiangwan@uio.no (Q. Wang), h.j.haugen@odont.uio.no (H.J. Haugen), dirk.linke@ibv.uio.no (D. Linke), s.p.lyngstadaas@odont.uio.no (S.P. Lyngstadaas), oes@landspitali.is (Ó.E. Sigurjónsson), qianlima@odont.uio.no (Q. Ma).

https://doi.org/10.1016/j.colsurfb.2025.114727
Received 14 March 2025; Received in revised form 17 April 2025; Accepted 19 April 2025
Available online 25 April 2025
0927-7765/© 2025 The Author(s). Published by Elsevier B.V. This is an open access article under the CC BY license (http://creativecommons.org/licenses/by/4.0/).

relies on maintaining a healthy peri-implant environment [6,7].

Several methods, including antibiotics, mechanical debridement, chemical cleaning, and combination approaches, have been proposed for managing peri-implantitis. Despite the available options, a consensus on the most effective therapeutic strategies remains elusive [8–10]. Chemical debridement agents are valuable adjuncts for cleaning implant surfaces, applicable in established and advanced peri-implant disease stages, and as preventive measures to maintain peri-implant health. Most of these agents only stay in situ for a short time and are removed within minutes of use. However, how these devices interfere with healing and regenerative treatments are not yet understood [11], emphasizing the need for a comprehensive evaluation of existing treatments and the development of new methodologies tailored explicitly for implant surfaces [12]. Supportive Peri-implant Care (SPIC) plays a crucial role in preventing disease recurrence or progression following peri-implantitis therapy [13–15]. Nevertheless, evidence is lacking to identify the most effective SPIC protocol and the role of adjunctive local antiseptic agents in secondary prevention, leaving also the optimal supportive care protocol yet to be determined [16,17].

Various debridement agents have also been assessed for their efficacy in treating biofilms on Ti implants. A review by Patil et al. identified chlorhexidine (0.2 %, CHX), citric acid (40 %), and sodium hypochlorite (1 %, NaClO) as the most commonly used chemotherapeutic cleaning agents [18]. High-quality evidence supports using CHX mouth rinse as an adjunct to mechanical hygiene, which significantly reduces dental plaque [19]. Cetylpyridinium chloride (0.05 %, CPC), an antimicrobial agent found in many toothpastes, provides 12-hour protection against plaque and gingivitis when used as a mouth rinse [20,21]. Poloxamer, a thermo-responsive hydrogel, has shown potential for alveolar bone regeneration and enhanced osteointegration, particularly when combined with mesenchymal stem cells (MSCs) or 1α,25-Dihydroxyvitamin D3 [22–24]. Additionally, its combination with H_2O_2 exhibits synergistic effects in Ti surface decontamination, utilizing oxidative and surfactant mechanisms to improve cleanliness [25,26].

Managing biofilm accumulation on Ti implant surfaces is essential to prevent peri-implant diseases and ensure implant longevity [27,28]. While chemical debridement agents are among the most effective methods for disrupting and removing biofilms, their impacts on peri-implant gingival tissues and bone regeneration still need to be better understood, with no current consensus in the literature [26]. This gap highlights the need to comprehensively evaluate these agents' biological effects on peri-implant tissues.

The long-term success of dental implants relies on both stable osteointegration and healthy peri-implant mucosal tissue. After implantation, bone marrow-derived mesenchymal cells (hBMSCs) are recruited to sites and differentiate into osteoblasts, initiating new bone formation on the implant surface [29,30]. Meanwhile, gingival fibroblasts (HGF), the main cellular component of the peri-implant connective tissue, contribute to soft healing and form a protective seal around the transmucosal region [31,32]. hBMSCs and HGFs were selected to model both hard and soft tissue responses *in vitro*. The MC3T3-E1 cell line was additionally used for its reproducibility and osteogenic behavior comparable to human primary osteoblasts [33].

This study systematically assessed the biological impact of various chemical debridement agents-H_2O_2, Poloxamer, H_2O_2 + Poloxamer, Perisolv (a commercial biofilm eraser containing 0.43 % sodium hypochlorite), and Gum Paroex® (a commercial product containing 0.12 % chlorhexidine gluconate and 0.05 % CPC)-on MC3T3-E1, HGF, hBMSCs cultured on OsseoSpeed®-like Ti surfaces, with saline as a control. The primary goal of this paper is to systematically evaluate the biological effects of the various chemical debridement agents on Ti implant surfaces after short-time exposure, focusing on their impact on cellular behavior, such as cell adhesion, proliferation, and viability that are essential for peri-implant tissue health and regeneration and dictate the clinical outcome of supportive peri-implant care and implant maintenance procedures.

2. Materials and methods

2.1. Materials preparation, surface characterization, and chemical debridement treatments

2.1.1. Preparation of OsseoSpeed™ surface topography of Ti coins

Ti coins (Grade II, 14 mm diameter, 1 mm height; Workshop, University of Oslo, Norway) were placed on silicone holders. One surface of each coin was blasted with TiO_2 particles (particle size:180–220 μm, F.J. Brodmann & Co., L.L.C., USA). The OsseoSpeed™ implant surface was prepared following the method described by Lamolle, S. F. [34].

2.1.2. Laser profilometer

The surface homogeneity of the Ti coins was assessed using a Profilometer (PLμ NEOX, Sensofar-Tech S.L., Terrassa, Spain). Images were captured at 150x magnification with a Nikon objective, obtaining five non-overlapping regions (85 x 63 μm^2). Surface parameters, including roughness, skewness, and kurtosis, were calculated using SensoMap Standard 6.2 software (Sensofar, Terrassa, Spain).

2.1.3. Chemical debridement agent treatment

The agents used for chemical debridement are listed in Table 1, with saline serving as the control. Agents were stored at 4 ℃ to maintain their liquid state and used at room temperature. Ti coins were disinfected with 75 % ethanol, air-dried, and placed in a 24-well tissue culture plate with the OsseoSpeed™ side facing up. Each coin was immersed in the agents for 2 minutes, rinsed with saline for 24 seconds, and vacuum suction was applied to remove residues. Prepared coins were then ready for cell seeding.

2.1.4. Fourier-transform infrared spectroscopy (FTIR)

The chemical composition of the Ti coin surface was analyzed using a PerkinElmer Spectrum 400 FT-IR/FT-NIR spectrometer (PerkinElmer, Waltham, MA, USA). Scans were performed in the mid-infrared region (4000–650 cm^{-1}) with a resolution of 2 cm^{-1} , using 256 scans per measurement. A background spectrum from a disinfected Ti coin was recorded as a reference. All samples were background-corrected, normalized, and analyzed using the Kubelka-Munk algorithm.

2.2. Cell experiment

2.2.1. Cell culture

MC3T3-E1 cells (ATCC, Manassas, VA, USA) were cultured in a complete medium containing low glucose Dulbecco′s Modified Eagle′s Medium (DMEM; Merck, Cat. No D5546) supplemented with 10 % fetal bovine serum (FBS) and 1 % penicillin-streptomycin (Gibco, Grand Island, NY, USA, Cat. No 15070–063). HGFs (Passage5–7, HFIB-G; Provitro, Berlin, Germany) were cultured in DMEM-low glucose with 10 % FBS, 1 % P/S, and 5 mM D-glucose. hBMSCs (Passage4–6, Ethics

TABLE 1
Agents used in the study.

Agent name	Content	Commercially usage
Control	0.9 % saline solution	
H_2O_2	3 % H_2O_2 in water (Sigma-Aldrich)	Generic compound
Poloxamer	28 % Poloxamer in water (Pluronic® F127, Sigma-Aldrich)	For wound caring [35]
H_2O_2 + Poloxamer	3 % H_2O_2 + 14 % Poloxamer	For peri-implantitis
Perisolv	0.43 % sodium hypochlorite/amino acid+hyaluronic acid (Perisolv®, Regedent AG)	Biofilm eraser
Paroex	0.12 % Chlorhexidine digluconate + 0.05 % Cetylpyridinium chloride (Gum Paroex®, Sunstar)	For mouth rinse

approval: Icelandic National Bioethics Committee, VSN19–189) were cultured in a DMEM/F12 with Glutamax (Gibco, Grand Island, NY, USA, Cat. No 31331–093), 10 % platelet lysate (PIPL, Bloodbank, Reykjavik, Iceland), 1 % P/S, and 2 IU/ml heparin (LEO Pharma A/Sm Ballerup, Denmark). Cells were incubated at 37 °C in a humidified incubator with 5 % CO_2. Cells were cultured in a medium with FBS/PIPL for proliferative activity, while for cytotoxicity assay and morphology, a medium without FBS/PIPL was used.

2.2.2. Cytotoxicity assay

Cytotoxicity was assessed using the LDH Cytotoxicity Detection Kit (Sigma-Aldrich, Cat. No 11644793001). Ti coins treated with agents were seeded with 4×10^4 cells per well in a 24-well tissue culture plate using the same complete medium without serum. After 30, 60, and 120 minutes, culture supernatants were collected for LDH assay according to the manufacturer's instructions. Absorbance was measured at 490 nm using a microplate reader.

2.2.3. Cell proliferative activity in response to different chemical debridement

Cell proliferation was evaluated using the Cell Counting Kit-8 (CCK-8; Abcam, ab228554). Following treatment with chemical agents, cells were seeded onto Ti coins in a 24-well tissue culture plate at a density of 3×10^4 cells per well (equivalent to 5000 cells per well in a 96-well plate) in a complete growth medium containing 10 % FBS. On days 1, 3, and 5, a 1:10 mixture of CCK-8 solution and growth medium was added to each well (600 μl/well), and the plates were incubated for another 4 hours. The media were then transferred to a 96-well plate (100 μl/well), and absorbance was measured at 460 nm using a microplate reader, reflecting cell proliferative activity indirectly.

2.2.4. Scanning electron microscopy (SEM)

Cells on the Ti surface were fixed with 2 % glutaraldehyde for 1 h at room temperature. Dehydration was carried out by immersing the samples sequentially in 30, 50, 70, 90, 100, 100 % ethanol, followed by incubation in 33, 66, and 100 % hexamethyldisilazane (HDMS, Sigma-Aldrich, Burghausen, Germany, Cat. No. 86944)/ethanol solutions for 20 min each round. The treated samples were then submerged in 100 % HDMS and left in a fume hood overnight to allow complete evaporation. After evaporation, the samples were sputter-coated with gold and images were captured by SEM (TM-1000, Hitachi, Tokyo, Japan).

2.2.5. Immunofluorescent staining and quantification

Following the treatment of agents, cells were seeded on Ti coins at a density of 4×10^4 cells per well in serum/PIPL-free culture medium and cultured for 30, 60, and 120 minutes. After fixation in 4 % paraformaldehyde for 15 minutes, cells were rinsed with PBS, permeabilized with 0.1 % Triton X-100 for 10 minutes, and blocked with 1 % BSA in PBS for 1 hour. Primary antibodies, including anti-phospho-FAK (Tyr861) (ThermoFisher, Cat. No 44–626G, 1:250) and anti-Vinculin antibody (Sigma, Cat. No V9131, 1:400), were incubated overnight at 4 ℃. After washing, samples were stained with Alexa Fluor 488-conjugated goat anti-rabbit secondary antibody and Alexa Fluor 488-conjugated goat anti-mouse secondary antibody (Invitrogen, Thermo Fisher Scientific, USA, 1:500) for 1 hour, respectively, followed by incubation with Alexa 568 Phalloidin (1:400) for 1 hour at room temperature. DAPI (300 nM in PBS) was used to counterstain nuclei for 15 minutes.

Images with Z-stack were captured by a laser scanning confocal microscope (Leica TCS SP8, Leica Microsystems, Wetzlar, Germany), and Z-projection images were generated. Cell outlines were manually traced, and the green channel (Alexa 488-labeled proteins) was isolated for semi-quantification. The green channel's integrated density (IntDen) was measured using ImageJ (version 1.4.3.67, National Institutes of Health, Bethesda, MD, USA). At the same time, cell mean diameter was calculated with Image Pro Plus (version 6; Media Cybernetics, Rockville, MD, USA) by outlining individual cells.

2.3. RNA-sequence analysis

2.3.1. Total RNA extraction

After treatment with agents in 24-well plates, 12 coins (4 x10^4 hBMSCs were seeded per coin) were used per agent group for RNA extraction. Three biological replicates were prepared per group. Total RNA was isolated using the RNeasy Mini Kit (QIAGEN, Cat. No 74104) following the manufacturer's instructions. RNA concentration was measured at 260 nm, and purity was assessed using the 260/280 nm and 260/230 nm ratio with a Nano-Drop ND 1000 Spectrometer (Wilmington, DE, USA).

2.3.2. Transcriptional profiling

Strand-specific TruSeq™ mRNA-Seq libraries were prepared from RNA samples and sequenced on the Illumina NovaseqX platform at the Norwegian Sequencing Centre (Oslo, Norway). FASTQ files from two sequencing lanes were merged for comprehensive data coverage. Low-quality read adapter sequences and PhiX spike-ins were removed using BBDuk (version 38, BBMap toolkit). Trimmed, paired-end reads were mapped to the human genome (GRCh38) with HISAT2 (version 2.2.1), producing SAM files, which were converted into BAM files with Samtools (version 1.2). BAM files were analyzed using featureCounts (version 2.0.1) and using GRCh38-derived gene annotation file to quantify unnormalized read counts. Differential expression analysis was performed in R (version 4.3.1) using DESeq2, with differentially expressed genes (DEGs) identified by an adjusted p-value (p.adj) threshold < 0.05.

2.3.3. GO and KEGG pathway enrichment

Gene Ontology (GO), Biological process (BP), and Kyoto Encyclopedia of Genes and Genomes (KEGG) pathway analyses were conducted to explore the functions of DEGs. GO BP enrichment categorizes genes by their biological functions, revealing their roles in various biological contexts. KEGG pathway analysis offers annotated genes involved in signal transduction and disease pathways, providing insights into the molecular pathways. Analyses were performed using resources from the Gene Ontology website (http://www.geneontology.org) and the KEGG database (http://www.genome.jp/kegg). Enrichment was considered statistically significant at an adjusted p-value (p.adj) < 0.05.

2.4. Statistical analysis

Unless otherwise noted, experiments were repeated three times, with at least three to four replicates per group. Data were analyzed using SPSS 28.0 (IBM, USA) and are presented as the mean ± standard deviation for continuous variables. Significant differences between groups were identified using one-way analysis of variance (ANOVA) followed by a Student-Newman-Keuls post hoc test for parametric data or Kruskal-Wallis tests followed by Dunn's multiple comparison tests for non-parametric data. Differences were considered statistically significant when $p < 0.05$. The data were plotted by Prism 9.4.1 (GraphPad Software, USA), with significant differences indicated by different letters (e.g., a, b, c; groups sharing a letter are not significantly different). Images and figures were formatted with Inkscape (version 1.3.2, Inkscape Project, https://inkscape.org/).

3. Results

3.1. Surface profile homogeneity detection of OsseoSpeed® like surface using FTIR

Ten randomly selected coins were evaluated for micro-topography. A profilometer scanned each coin at five non-overlapping points. No statistically significant differences in roughness, skewness, or kurtosis were shown among the coins (Supplement Fig.1).

Most debridement agents were easily removed from the Ti surface

using room-temperature saline (20 ℃). However, Poloxamer solidified upon contact with the Ti surface, making it resistant to complete removal and leaving reminiscence behind. Cold saline (4 ℃) effectively eliminated it. FTIR analysis identified functional groups on the Ti surface, with wavenumber (cm^{-1}) on the X-axis representing reflecting molecular vibrations and percent reflectance (%R) on the Y-axis indicating infrared absorption intensity. After room-temperature saline flushing (Fig. 1, red line), Poloxamer exhibited characteristic peaks: O-H stretching (3487 cm^{-1}), -CH stretching (2906 cm^{-1}), -CH2 bending (1471 cm^{-1}), and C-O-C stretching (1157 cm^{-1}), corresponding to polyethylene oxide (PEO) and polypropylene oxide (PPO) segments in Pluronic® F127 [36]. These peaks disappeared after cold saline flushing (Fig. 1**C**).

3.2. Agent cytotoxicity and cellular adhesion, morphology, and proliferation

3.2.1. Experiments performed on MC3T3-E1 cell line

3.2.1.1. Cell adhesion, cytotoxicity, proliferation. Poloxamer-treated Ti surfaces significantly enhanced MC3T3-E1 adhesion at all time points (Supplement Fig.2A, B, $p < 0.05$). Elevated LDH activity was observed only in the Paroex group ($p < 0.05$) (Supplement Fig.2**C**). On day 1, Perisolv and Paroex promoted proliferation compared to the control. By day 3, Perisolv maintained this effect, while H_2O_2 + Poloxamer and Paroex inhibited proliferation. By day 5, all treatments inhibited proliferation except Poloxamer, which consistently showed the highest proliferation across all time points (Supplement Fig.2**D**, $p < 0.05$). Cells on saline- and Poloxamer-treated Ti had the largest mean diameters, while those in the Perisolv and Paroex groups had the smallest (Supplement Fig.3**D**).

3.2.1.2. pFAK & Vinculin intensity. At 30 minutes, pFAK and Vinculin immunofluorescent intensities showed no significant differences between groups. By 60 minutes, pFAK intensities were highest in the control and Poloxamer groups, while other groups showed reduced levels. Vinculin intensities were similarly reduced in the H_2O_2 + Poloxamer, Perisolv, and Paroex groups. At 120 minutes, all groups except Poloxamer showed decreased pFAK and Vinculin intensities, with Poloxamer maintaining levels comparable to the control (Supplement Fig.3**B, C**, $p < 0.05$).

Additionally, after cold saline flushing, Poloxamer treatment no longer enhanced MC3T3-E1 adhesion or spreading, as the gel was removed entirely (Supplement Figs.4–5, Fig1**.C**).

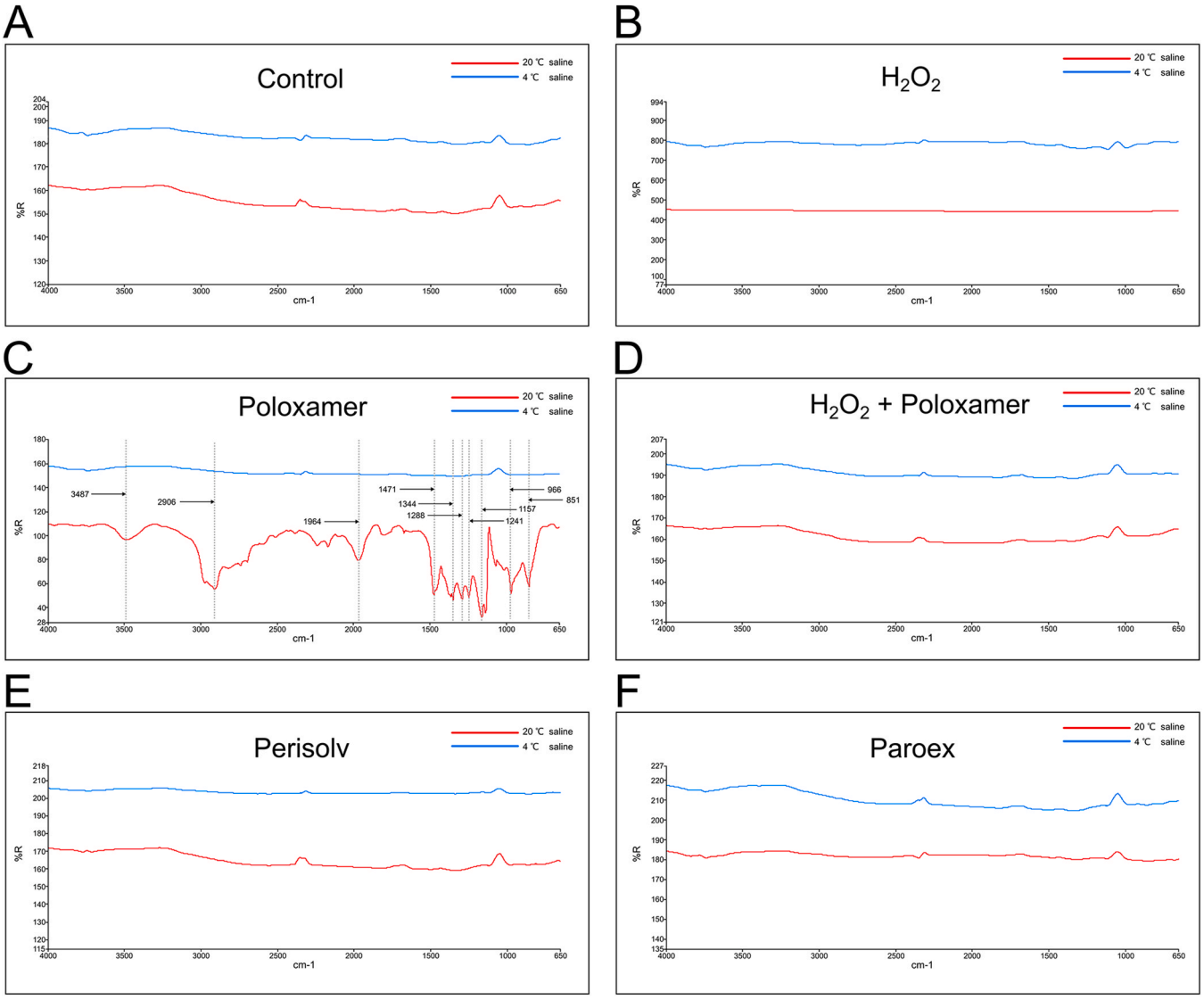

Fig. 1. FTIR spectra of Ti implant surfaces after chemical debridement treatment. (A) Control; (B) H_2O_2; (C) Poloxamer; (D) H_2O_2+Poloxamer; (E) Perisolv; (F) Paroex.

3.2.2. Experiment performed on HGF cell line

3.2.2.1. Cell adhesion, cytotoxicity, proliferation. Significantly more HGF cells adhered to Poloxamer-treated Ti surfaces at all time points, while the Paroex -treated surfaces showed the fewest adherent cells (Fig. 2**A, B**, $p < 0.05$). Elevated LDH activity was observed only in the Paroex group at 60 and 120 minutes (Fig. 2**C**, $p < 0.05$). On days 1 and 3, Poloxamer and Perisolv supported proliferation rates comparable to the control, while other treatments inhibited proliferation. By day 5, all treated surfaces reduced proliferation compared to the control, but Poloxamer and Perisolv supported higher proliferation than H_2O_2, H_2O_2 + Poloxamer, and Paroex (Fig. 2**D**, $p < 0.05$). HGF cells on Poloxamer-treated surfaces had the largest mean diameters among non-control groups across all time points (Fig. 3**D**, $p < 0.05$).

3.2.2.2. pFAK & Vinculin intensity. At 30 minutes, pFAK intensity was highest in the H_2O_2 + Poloxamer group, followed by the Perisolv, both exceeding the control ($p < 0.05$). By 60 and 120 minutes, the Poloxamer group showed the strongest pFAK signal among non-control groups. For Vinculin intensity, the Paroex group had the highest signal at 30 minutes, while Poloxamer had the strongest signal at 60 and 120 minutes among non-control groups (Fig. 3**B, C**, $p < 0.05$).

3.2.3. Experiments performed on hBMSC cell line

3.2.3.1. Cell adhesion, cytotoxicity, proliferation. hBMSC adhesion followed a pattern like MC3T3-E1 and HGF cells, with the Poloxamer group showing the highest adhesion among experimental groups (Fig. 4**A, B**, $p < 0.05$). LDH activity was significantly elevated in the H_2O_2 and H_2O_2 + Poloxamer groups at 30 and 60 minutes, peaking in the H_2O_2 + Poloxamer group at 120 minutes, followed by the Paroex (Fig. 4**C**). Proliferation was reduced in all experimental groups compared to the control. On days 1 and 5, the Poloxamer group had the highest proliferation among experimental groups. In contrast, on day 3, the H_2O_2, Poloxamer, and Paroex groups showed comparable proliferation levels, exceeding H_2O_2 + Poloxamer and Perisolv (Fig. 4**D**, $p < 0.05$). Cell mean diameters were similar across groups at 30 minutes. By 60 minutes, the control group had the largest diameter, while Perisolv-treated cells had the smallest. At 120 minutes, the control and Poloxamer groups exhibited the largest diameter (Fig. 5**D**, $p < 0.05$).

3.2.3.2. pFAK & Vinculin intensity. pFAK intensities showed no significant differences across groups at 30 minutes. At 60 minutes, only the Perisolv group reached control-equivalent levels. By 120 minutes, the control and Poloxamer groups exhibited the highest pFAK intensities (Fig. 5**B**, $p < 0.05$). The Paroex group had the highest levels of Vinculin intensities at 30 minutes. At 60 minutes, the H_2O_2 and Perisolv groups

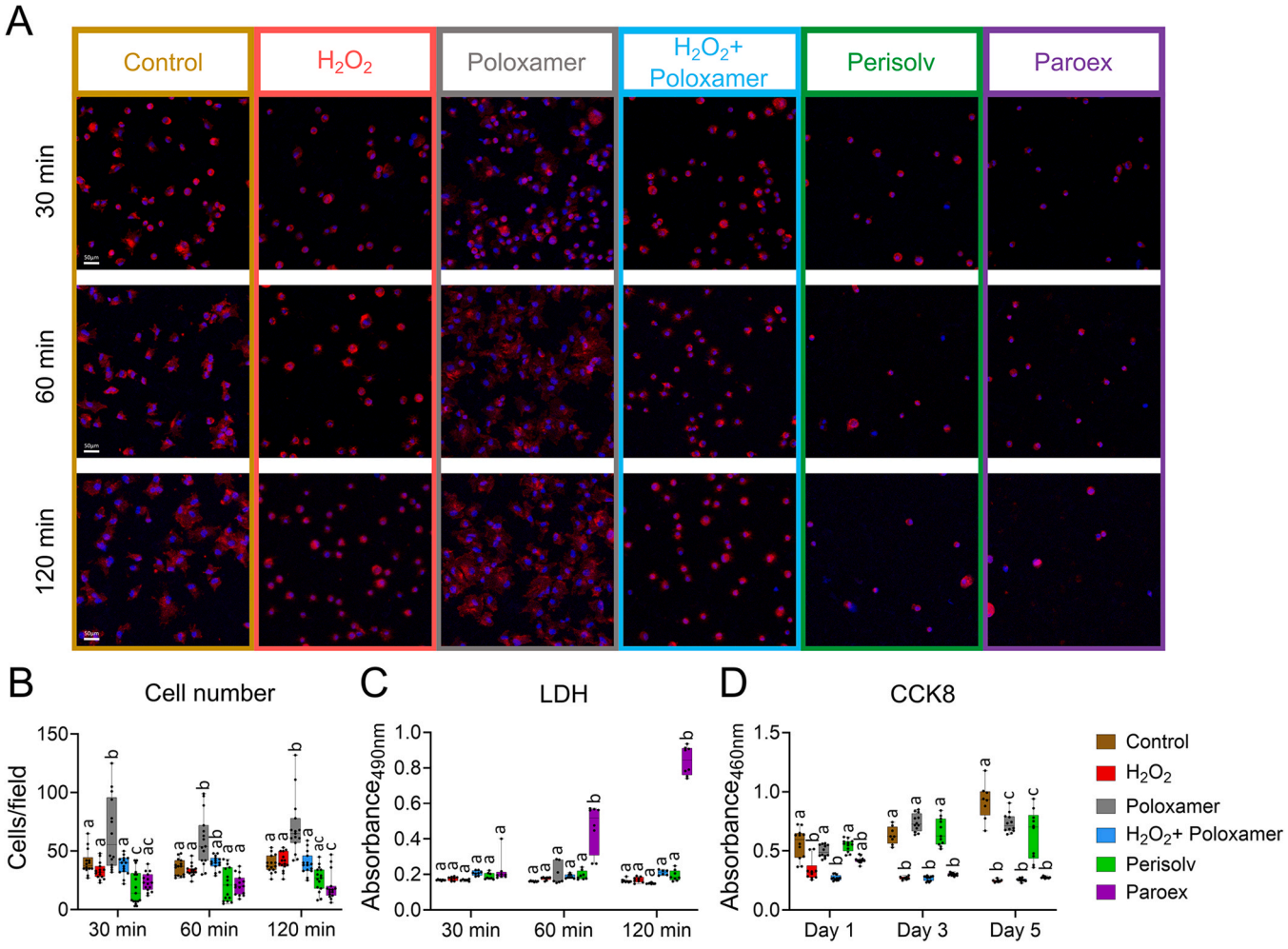

Fig. 2. Biological behavior of HGFs on Ti implant surfaces after chemical debridement treatment. (A) Confocal microscopic inspection of F-actin (red) and DAPI (blue) stained in cells seeded on pretreated Ti surfaces at different time points; (B) Semi-quantitative analysis of cells attached on pretreated Ti surfaces at different time points; (C) LDH release from cells on pretreated Ti surfaces at different time points; (D) Cell proliferative activity on pretreated Ti surfaces at day 1, 3 and 5. Statistical significance is indicated by different letters (a, b, c, etc.), as described in the statistical analysis section. Scare bar = 50 μm.

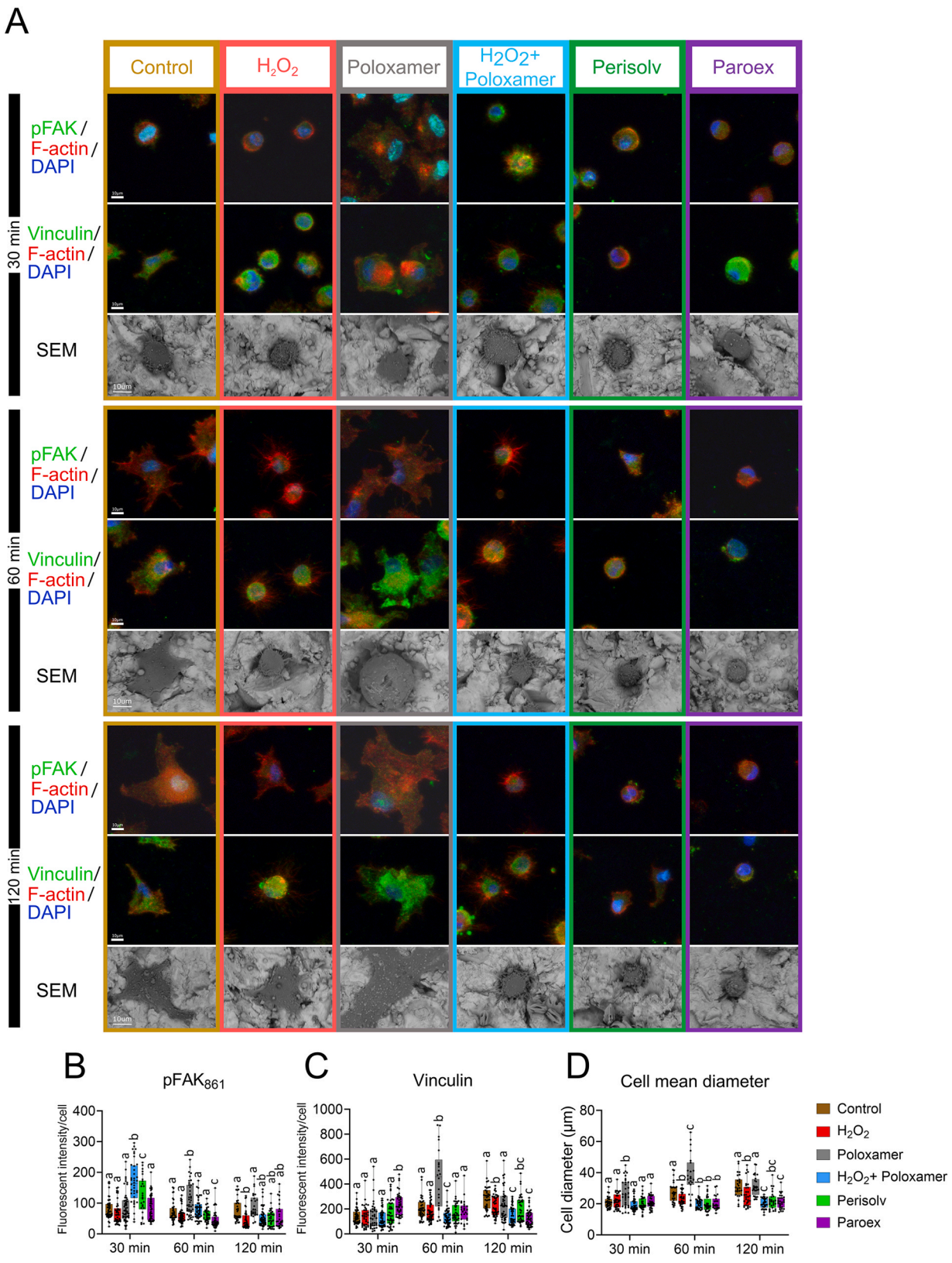

Fig. 3. Attachment behavior of HGFs on Ti implant surfaces after chemical debridement treatment. (A) Confocal microscopic inspection of pFAK (green), Vinculin (green), F-actin (red), and DAPI (blue) staining of cells seeded on pretreated Ti surfaces at different time points; (B) Semi-quantitative analysis of pFAK expression per cell at different time points; (C) Semi-quantitative analysis of Vinculin expression per cell at different time points; (D) Mean diameter of cells on pretreated Ti surfaces at different time points. Significance is indicated by different letters (a, b, c, etc.), as described in the statistical analysis section. Scare bar = 10 μm.

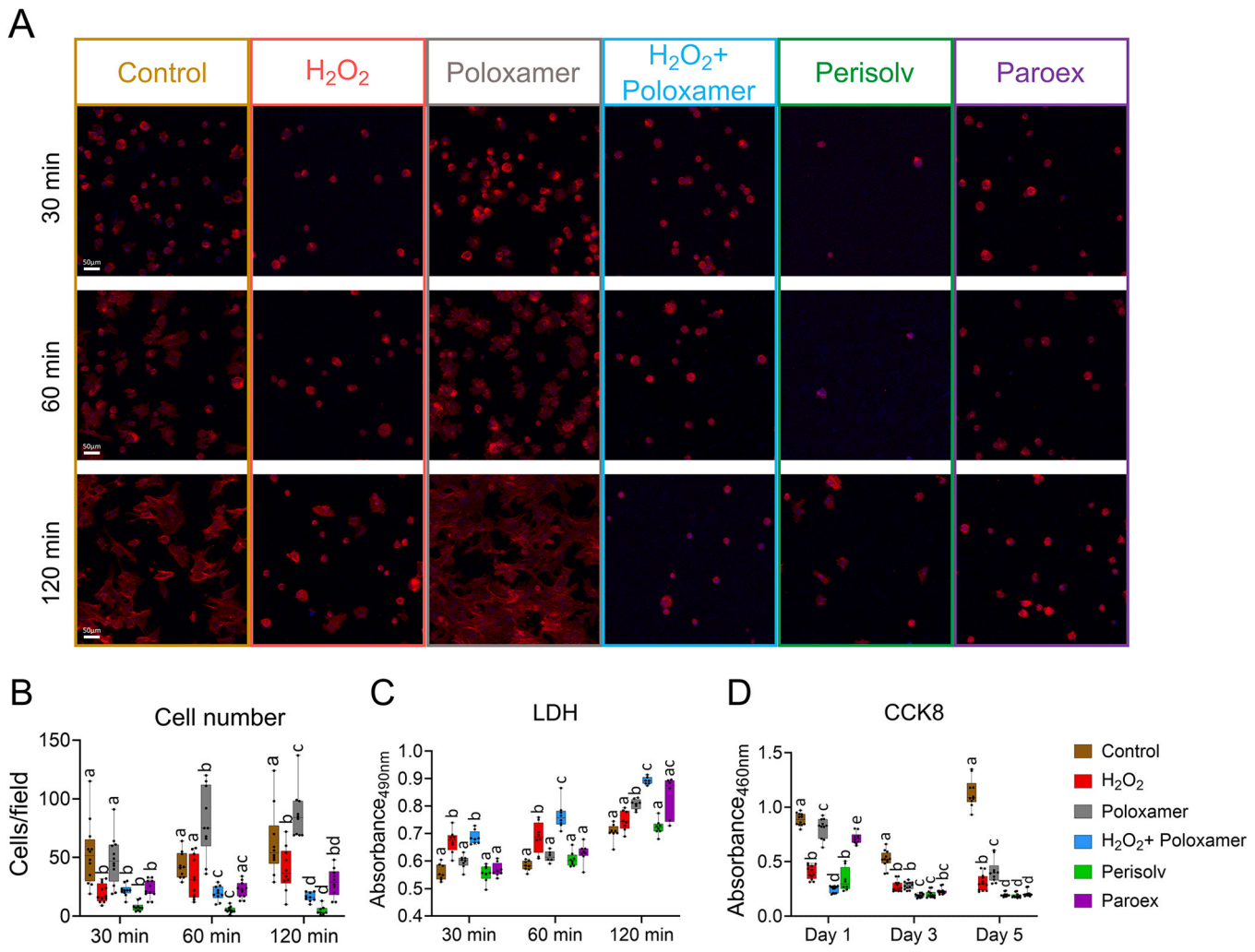

Fig. 4. Biological behavior of hBMSCs on Ti implant surfaces after chemical debridement treatment. (A) Confocal microscopic inspection of F-actin (red) and DAPI (blue) stained in cells seeded on pretreated Ti surfaces at different time points; (B) Semi-quantitative analysis of cells attached on pretreated Ti surfaces at different time points; (C) LDH release from cells on pretreated Ti surfaces at different time points; (D) Cell proliferative activity on pretreated Ti surfaces at day 1, 3 and 5. Statistical significance is indicated by different letters (a, b, c, etc.), as described in the statistical analysis section. Scare bar = 50 μm.

displayed reduced intensities, while at 120 minutes, the Perisolv showed the lowest Vinculin intensity, with no significant differences among other groups (Fig. 5**C**).

3.3. Gene expression profile

RNA sequencing data showed high alignment rates with Hisat2 and effective fragment assignment via featureCounts, confirming high-quality sequencing (Supplement Table 1). Principal component analysis (PCA) revealed distinct sample clustering by treatment. Debridement agents primarily influenced PC1 (74 % variance), while PC2 (12 % variance) reflected finer biological or technical distinctions. Saline (control) and Poloxamer-treated samples cluster closely along PC1 and PC2, suggesting similar transcriptional profiles, as did the H_2O_2 + Poloxamer and Perisolv groups (Fig. 6**A**).

A Venn diagram of DEGs (log_2FoldChange >1, $p.adj < 0.05$) showed only 293 DEGs were uniquely shared between the H_2O_2 + Poloxamer and Poloxamer groups, while 2523 DEGs uniquely shared between the H_2O_2 + Poloxamer and Perisolv groups, indicating relatively similar gene expression profiles, consistent with PCA (Fig. 6**B**). A heatmap of the top 500 DEGs (lowest p.adj) revealed clustering patterns, with H_2O_2 + Poloxamer and Perisolv grouping together, and H_2O_2 and Paroex forming another cluster (Fig. 6**C**). Additional analysis, including volcano plots, and heatmaps, are available in Supplement Fig. 6.

GO enrichment analysis ($p.adj < 0.05$) revealed the impact of agent treatments on cellular biological processes.

All debridement agents, except Poloxamer, activated apoptotic signaling pathways compared to the control. Oxidant-based debridement agents (H_2O_2, H_2O_2 + Poloxamer, Perisolv) notably downregulated biological processes related to cell-substrate adhesion and junction organization (Fig. 7**A**). It was found in further analysis, key genes within apoptosis, proliferation, cell-adhesion processes were affected. Specifically, proliferation-regulatory genes (*NOTCH1*, *JAG1*, *HMGA2*, *YAP1*, *TBX3*), anti-apoptosis genes (*MCL1*, *BCL2L2*), and cell-substrate adhesion genes (*ITGA2*, *ITGB3*, *SPP1*) showed marked downregulation.

KEGG enrichment analysis ($p.adj < 0.05$) identified several significantly enriched pathways associated with agent treatments. Oxidant-based agents significantly inhibited MAPK signaling, PI3K-Akt signaling, and focal adhesion pathways. Apoptosis was exclusively activated by H_2O_2 and H_2O_2 + Poloxamer treatment. Key components of the MAPK pathway (including *MAPKAPK2*, *NRAS*, and *KRAS*) were downregulated following oxidant-based debridement, which also suppressed the PI3K-Akt signaling pathway (Fig. 8).

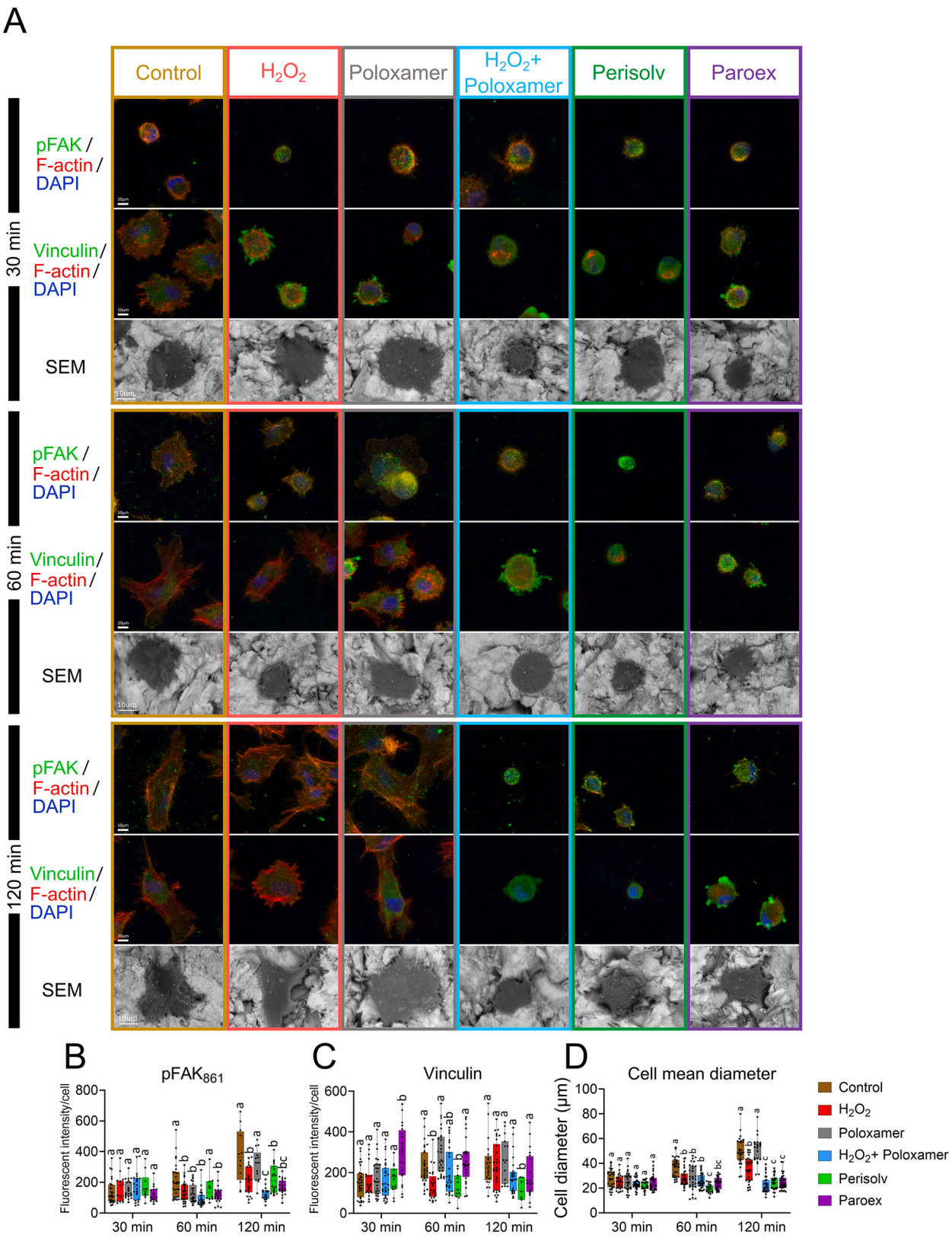

Fig. 5. Attachment behavior of hBMSCs on Ti implant surfaces after chemical debridement treatment. (A) Confocal microscopic inspection of pFAK (green), Vinculin (green), F-actin (red), and DAPI (blue) staining of cells seeded on pretreated Ti surfaces at different time points; (B) Semi-quantitative analysis of pFAK expression per cell at different time points; (C) Semi-quantitative analysis of Vinculin expression per cell at different time points; (D) Mean diameter of cells on pretreated Ti surfaces at different time points. Significance is indicated by different letters (a, b, c, etc.), as described in the statistical analysis section. Scare bar = 10 μm.

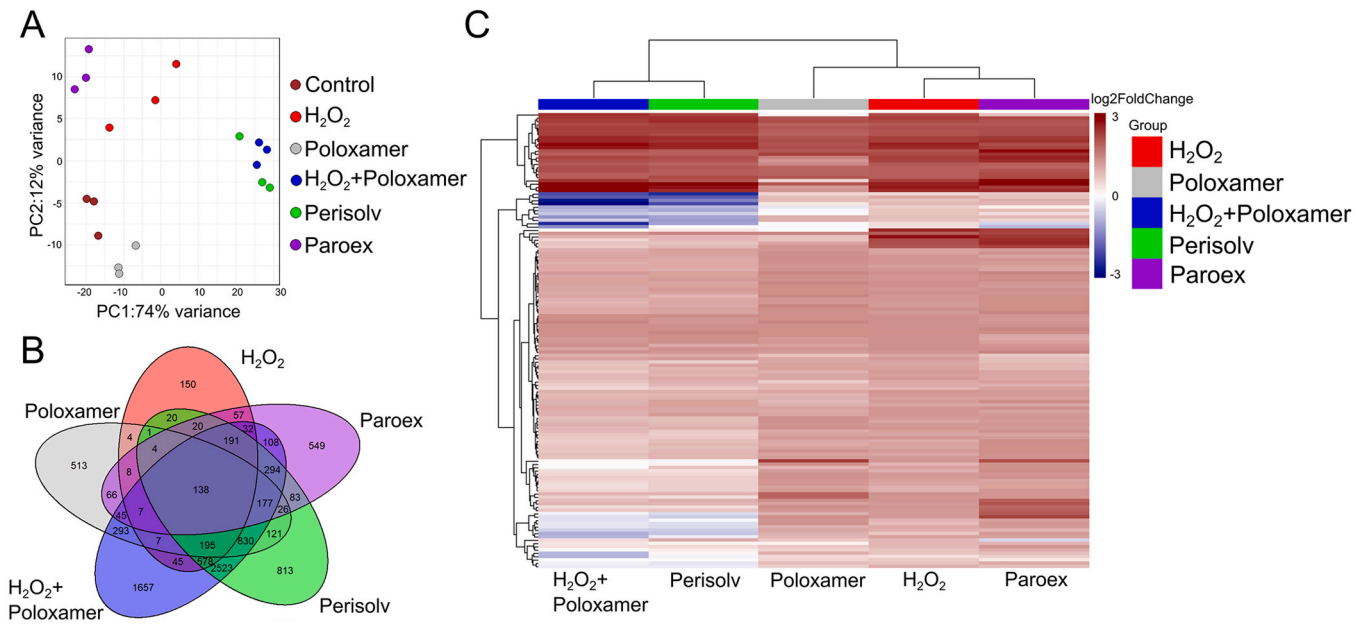

Fig. 6. Comprehensive analysis of differentially expressed genes (DEGs) across experimental conditions. (A) Principal component analysis (PCA) across all chemical debridement with all independent samples; (B) Venn diagram of DEGs overlap across control-based comparisons; (C) Heatmap of top 500 DEGs across control-based comparisons with hierarchical clustering. DEGs were screened by $p.adj < 0.05$. $\log_2$FoldChange values were centralized and shown in a range from −3 (down-regulated) to 3 (up-regulated).

4. Discussion

Chemical cleaning agents are commonly used for implant surface decontamination, but their effects on peri-implant gingival tissues and bone regeneration remain obscure. Re-osseointegration of implants requires cells to attach fast and well to implant surfaces, but there is no agreement on which debridement methods work best prior to regenerative measures [26,37]. This study systematically evaluated the biological effects of chemical debridement agents on MC3T3-E1, HGF, and hBMSCs cultured on Ti implant surfaces, focusing on initial cellular responses within 120 minutes, building upon our preliminary experiments and a previous study that analyzed cell morphology on Ti surfaces [38]. Among the agents tested, Poloxamer showed the highest biocompatibility. In contrast, all other agents impaired hBMSCs' adhesion, spreading, and proliferation on Ti surfaces with apparent cytotoxicity. However, Poloxamer partially rescued H2O2-induced inhibition of ossification, epithelial cell proliferation, and hemopoiesis at the transcriptional level. Such impaired biofunctions of hBMSCs were evident from reduced expression of key adhesion molecules, such as phosphorylated adhesion kinase (pFAK) and Vinculin, which are critical for focal adhesion formation and cell attachment to biomaterial's surface [39,40]. As a key precursor of osteoblastic lineage cells, the rapid adhesion and osteogenic differentiation of hBMSCs to the implant surface is essential for the primary success of dental implant treatment and also perform as a prerequisite for the success of peri-implantitis treatment [41,42]. Such findings raise concerns about the debridement agents commonly used in clinical practice, which cause detrimental effects on the survival and osteogenic activity of hBMSCs, thereby hindering the acquisition of a regenerative environment after chemical debridement.

Theoretically, if the cleaning agent can be removed entirely after the debridement procedure, the cytotoxicity caused by residual components can be avoided. However, in practice, the treatment of peri-implantitis is often complicated by deep or irregular periodontal lesions, which can trap residues of the debridement agent. This study reflects the clinical reality that some debridement agents can remain behind. In detail, the toxic and inhibitive effects of Paroex treatment on the Ti implant surface are likely due to residual CHX, the main active ingredient in Paroex, staying on the plates after rinsing and likely leaching back into the medium during cell seeding. CHX has been shown to disrupt the actin cytoskeleton, reduce cell adhesion, and impair osteoblast viability. Previous studies reported that 0.12 % CHX hindered re-osseointegration in canine peri-implantitis models, with new bone forming at a distance from the implant surface [43]. Additionally, CHX exposure has been associated with necrotic cell death, apoptosis in osteoblasts [44], and downregulation of genes related to matrix components and cell adhesion receptors in HGF [45]. Since, in our hands, Paroex inhibited hBMSCs adhesion, spreading, and proliferation with significant cytotoxicity, it may not be suitable for routine use in peri-implant biofilm removal or peri-implant health maintenance at all.

Regarding the high abundance of anaerobes and facultative anaerobes in the peri-implant inflammatory microenvironment, applying peroxide may constitute an effective strategy to maintain peri-implant health [46]· H_2O_2 and H_2O_2 + Poloxamer were used in this study as chemical debridement agents because of their convenient availability and ideal biosafety (3 % hydrogen peroxide has been widely used in dental clinical treatment for a long time) [47,48]. However, even as one of the least active reactive oxygen species (ROS), H_2O_2 can still induce cell death when its concentration exceeds the antioxidant capacity of cells [49]. In this study, H_2O_2 and H_2O_2 + Poloxamer did not exhibit cytotoxicity or impair the adhesion of MC3T3-E1 and HGF to Ti implant surfaces. Still, they showed cytotoxicity to hBMSCs, as evidenced by reduced adhered cell numbers and elevated LDH levels. These observed differences indicate that hBMSCs are more sensitive to H_2O_2 than MC3T3-E1 and HGF.

The mechanisms of H_2O_2-induced cytotoxicity vary across cell types, leading to diverse responses at different concentrations [50]. Previous studies have shown that low concentrations (200–300 μM) of H_2O_2 impair the stemness of BMSCs with compromised differentiation potentials [51]. Another study revealed that residual H_2O_2 in equipment after steam disinfection significantly reduced cell proliferation and survival in a dose-dependent manner. Specifically, concentrations above 0.5 mg/L (14.7 μM) affected cell viability, and at 5.0 mg/L (147 μM), hBMSCs were completely eliminated [52]. Interestingly, while 200 μM H_2O_2 suppressed proliferation in the mouse osteoblastic cell line (MC3T3-E1) and human osteoblast-like cell line (MG63), cell viability remained unaffected [53,54]. Similarly, the proliferation of HGFs was

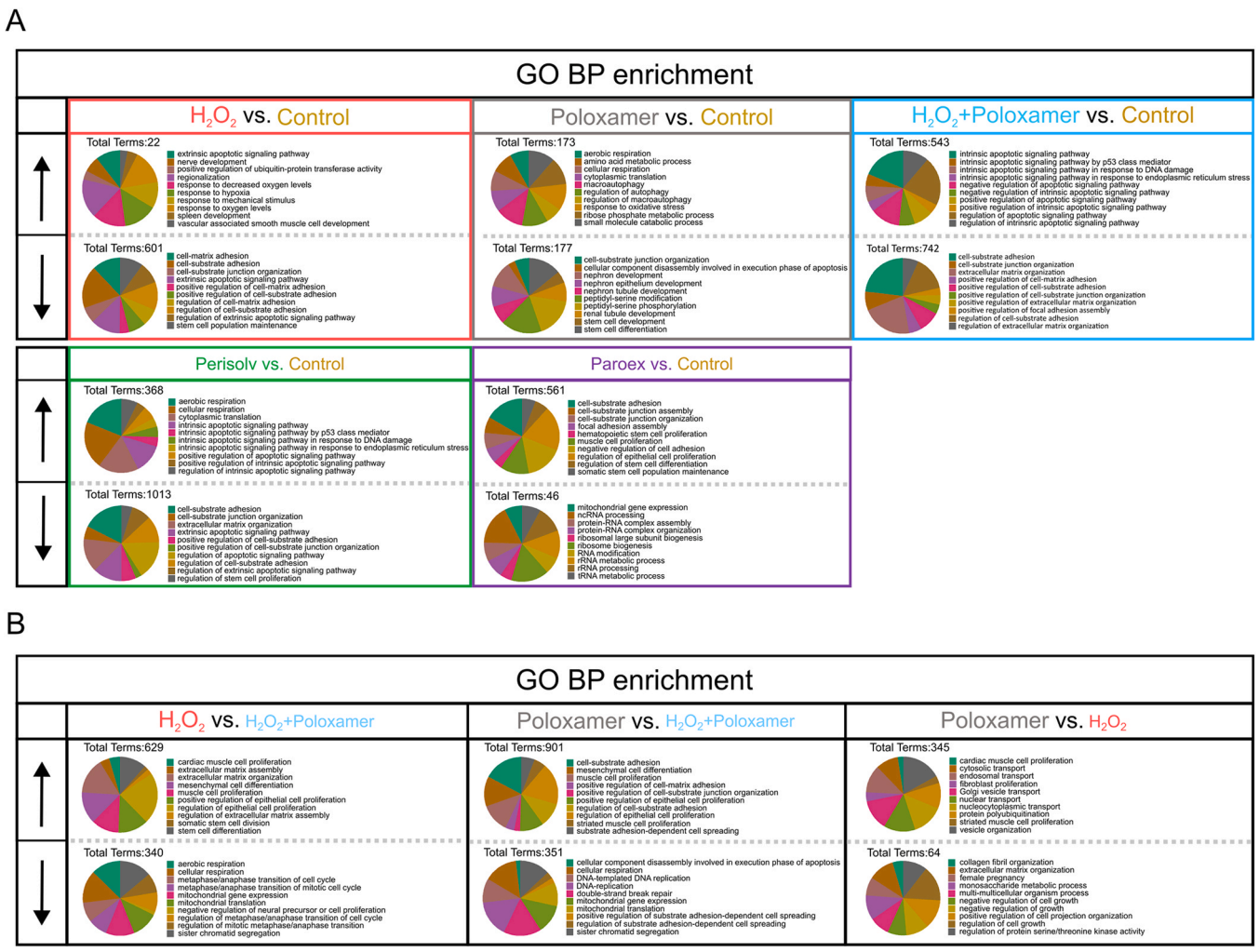

Fig. 7. Gene Ontology (GO) Biological Process (BP) enrichment analysis for pairwise comparisons. (A) Top 10 enriched GO BP terms for control-based pairwise comparisons. Pie charts prioritize three key functional categories: apoptosis, proliferation, and extracellular matrix organization/cell-substrate interactions, followed by additional terms ranked by gene count. (B) Similar representation for three non-control-based pairwise comparisons, highlighting the same functional categories. Upregulated and downregulated terms are indicated by up and down arrows, respectively.

inhibited at the same concentration, but no significant cell death was observed [55]. These findings suggest that MC3T3-E1 and HGFs have a higher tolerance to H_2O_2-induced cytotoxicity compared to BMSCs, supporting our results that low concentration of H_2O_2 primarily inhibited proliferation, with notable cytotoxic effects specific to hBMSCs. This highlights the greater sensitivity of hBMSCs to H_2O_2 compared to MC3T3-E1 and HGFs.

In our study, residual trace amounts of H_2O_2 at the microspace between the coin and the 24-well plate, undetectable by FTIR but leaching into the medium during cell seeding, may impair cell viability and spread despite apparent surface cleanliness. However, in a peri-implantitis clinical setting, the hydrogen peroxide would likely have been used up due to the biofilm presence and its organic components. Therefore, what is presented here is a "worst-case scenario" of chemical debridement agents to hBMSCs. Such a hypothesis was also supported by the impaired biocompatibility of Ti implant surfaces after the Paroex treatment. Similarly, NaClO (0.43 %) in Perisolv may have similar adverse effects for the same reason. Interestingly, while Perisolv (containing NaClO) didn't inhibit the proliferation of MC3T3-E1 and HGFs on day 1 and day 3, it consistently impaired proliferation in hBMSCs from day 1 onward, indicating a cell type-specific sensitivity. As a commonly used oxidative disinfectant in endodontic treatment, NaClO can generate ROS inside microbes, and its toxicity arises from its corrosive activity [56]. Nevertheless, the contradiction between hBMSCs, MC3T3-E1, and HGFs suggests that the cytotoxicity elicited by NaClO may not be attributed to direct corrosion. ROS generated by oxidative disinfectants applied in this study are more toxic to hBMSCs adapted to the anaerobic environment in the bone marrow and may further impair their osteogenesis-related functions [51]. Notably, H_2O_2 has increased DNA damage markers in senescent BMSCs [57]. Consistent with this, our GO enrichment analysis revealed that both H_2O_2 and NaClO activate DNA damage pathways, such as 'signal transduction in response to DNA damage' and 'intrinsic apoptotic signaling pathway in response to DNA damage'. Notably, the anaerobic environment of peri-implantitis lesions can rapidly consume residues of oxidative debridement agents, thereby alleviating oxidative stress on hBMSCs. However, the negative impact of trace oxidants on the bioactivity of Ti implant surface and tissue regeneration peri-implant should be considered. Further research is needed to clarify whether oxidative debridement agents can hinder tissue regeneration by altering the characteristics of Ti implant surfaces.

Besides the adverse effects of the abovementioned agents, Poloxamer exhibited an optimistic performance in the regenerative functions of all three tested cells. These effects are attributed to Pluronic 127, the primary component of Poloxamer, an ABA-type triblock copolymer that can change from liquid to gel state with increased temperature. Poloxamer is known as a stable hydrogel and osteoconductive scaffold, promoting bone regeneration and wound healing [35,58]. Its resemblance to the extracellular matrix (ECM), high water content, porosity, and

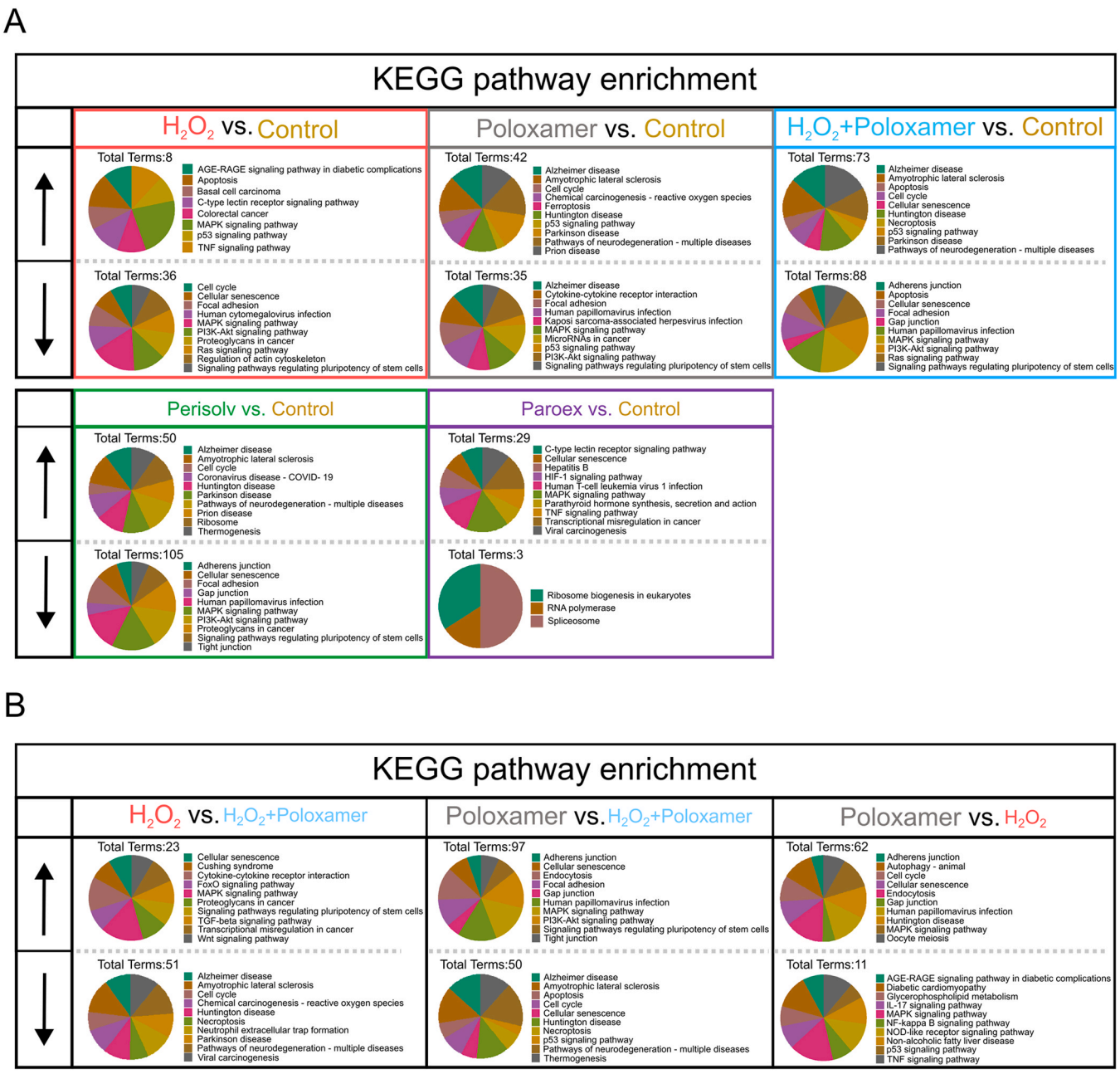

Fig. 8. KEGG enrichment analysis for pairwise comparisons. (A) Top 10 enriched KEGG pathways for control-based pairwise comparisons. Pie charts prioritize three key functional categories: cell growth and death, immune system, and cellular community – eukaryotes, followed by additional pathways ranked by gene count. (B) Similar representation for three non-control-based comparisons, highlighting the same functional categories. Upregulated and downregulated pathways are indicated by up and down arrows, respectively.

structural flexibility enhance BMSC viability and ECM protein interactions [59]. Its positive bioactivities and rapid transformation into colloid after being applied to peri-implant lesions are conducive to its local effect. When applied together with H_2O_2, it also acts as an excipient to facilitate the retention of H_2O_2 in-situ. Additionally, Poloxamer improves cellular affinity, maintains osteoblast activity *in vitro*, and reduces pro-inflammatory cytokine expression in the local milieu, resulting in a milder inflammatory response than surgical suture materials. Compared with the periodontal tissue structure of natural teeth, the poor sealing between the implant and the soft tissue surrounding it leads to bacterial invasion and inflammatory destruction of the implant-osseointegration interface [60]. Routine application of non-invasive chemical debridement to remove infection and reactivate the peri-implant regenerative microenvironment may serve as an effective health control strategy for implant treatment. Poloxamer's ideal biocompatibility and inflammation modulating effect highlight the potential as a promising chemical debridement agent for peri-implantitis treatment and peri-implant health support and maintenance.

Most studies on preventing and treating peri-implantitis employed conventional research technologies for biochemical detection, such as ELISA and PCR [61–63], which provided limited information restricted to individual biomarkers. This study utilized sequencing technology to systematically analyze the whole transcriptome of hBMSCs on Ti implant surfaces following treatment with different chemical debridement agents. This approach facilitates the identification of the direct impact of chemical debridement strategies on genes and molecules associated with peri-implant tissue regeneration. Furthermore, it lays a solid experimental foundation for exploring and developing reactivation

agents' post-debridement targeting specific signaling pathways. The GO biological process enrichment analysis results in this study indicate that oxidant-based debridement significantly inhibited hBMSC proliferation. Specifically, key regulatory genes, including *NOTCH1, JAG1*, *HMGA2*, *YAP1*, and *TBX3*, were markedly downregulated. Previous studies have shown that downregulation of these genes leads to compromised cellular proliferation. For instance, MSC proliferation is accelerated under hypoxia by increasing *NOTCH1* expression, while *JAG1*-mediated *NOTCH* signaling and upregulated *HMGA2* expression both promote hBMSC proliferation. Similarly, the upregulation of *YAP1* and *TBX3* has been associated with enhanced cellular proliferation [64–68]. Furthermore, anti-apoptosis genes such as *MCL1* and *BCL2L2* showed reduced expression. While the downregulation of these genes could be beneficial in targeting cancer cells, it may compromise normal cell survival [69, 70]. Expression of cell-substrate adhesion genes, such as *ITGA2, ITGB3*, and *SPP1*, was also inhibited, which is undesirable as it could impair cell adhesion (Fig. 7) [71–73]. KEGG enrichment analysis revealed significant downregulation of the MAPK signaling pathway (including *MAPK*, *APK2*, *NRAS*, and *KRAS*) and suppression of the PI3K-Akt signaling pathway following oxidant-based debridement treatment. Notably, focal adhesion functions *(ITGA2*, *ITGB3*, *SPP1*, *ROCK1*, *PIK3CA*, *CRK*, *PDGFRA*) were also diminished (Fig. 8). Our gene expression analysis data suggest that hBMSCs on Ti surfaces experience challenges in adhesion and survival at early time points, potentially compromising their regenerative capacity. Prolonged exposure to these oxidant-based agents may result in sustained cellular stress, potentially manifesting as reduced proliferation, increased apoptosis, and diminished differentiation capacity. Consequently, this could significantly impair the ability of hBMSCs to contribute effectively to tissue regeneration in peri-implantitis lesions.

5. Limitation

This study still has some shortcomings that need further research in the future. Firstly, the Ti implant surfaces were kept aseptic and free of saliva components, which could not fully replicate the clinical reality where saliva, microorganisms, and proteins adhere to implant surfaces. Osteoblastic behavior and function were compromised on Ti surfaces contaminated with saliva [74,75]. In clinic peri-implantitis, anaerobic bacterial such as *Porphyromonas gingivalis*, *Tannerella forsythia*, *Treponema denticola*, and *Fusobacterium nucleatum* contribute to disease progression through complex biofilm and heightened inflammation responses. Future studies should incorporate anaerobic conditions to replicate the clinical environment better and explore the interactions between debridement agents, peri-implant cells, and anaerobic microbiota [46]. In addition, this static model is challenging to simulate the continuous flushing of the patient's gingival crevicular fluid, which can effectively reduce the toxicity of the residual chemical debridement agent. A dynamic biofilm model constructed with pathogenic bacteria of peri-implantitis would be more appropriate to replicate the peri-implant condition. To reestablish adequate peri/implant health around infected implants, a chemical debridement agent should be applied for a short term and removed, followed by a bioactive biomaterial, like commercially available Emdogain® or hyaluronic acids [76–78], that has the potential for inducing healing and growth of peri-implant tissues.

6. Conclusion

Several chemical debridement agents effectively remove biofilms from infected dental implant surfaces. However, the biological effects of these agents have not yet been fully investigated. Of the tested materials, Poloxamer showed the best biocompatibility for use on Titanium implant surfaces. This mild cleaning agent supported cell adhesion and proliferation, and induced expression of molecules known to be important in peri-implant tissue regeneration. Commercial agents such as Perisolv and Paroex inhibited hBMSCs' adhesion, spreading, and proliferation, with Paroex demonstrating significant cytotoxicity, raising concerns about their routine clinical use. H_2O_2 treatment exhibited cytotoxic effects, particularly against hBMSCs, which were more sensitive to H_2O_2 than MC3T3-E1 and HGF cells. Oxidant-based debridement agents increased apoptosis while inhibiting proliferation, cell-substrate adhesion, focal adhesion pathways, and signaling pathways regulating pluripotency in stem cells.

These findings underscore the importance of carefully selecting and optimizing debridement agents to balance antimicrobial efficacy and cytocompatibility, particularly in cases of peri-implantitis and peri-mucositis. Since several of the chemical cleaning agents investigated caused cellular harm to hBMSCs, complete and quick removal after cleaning seems crucial.

This study emphasizes the need for ongoing innovation in implant decontamination strategies and a deeper understanding of the interplay between debridement strategies, implant surfaces, and peri-implant tissues, ultimately providing the basis for evidence-based, clinical practices and optimizing Supportive Peri-implant Care protocols.

Funding statement

This study was supported by the Research Council of Norway ('MISFAITH' grant no. 331752; 'Debrigel' grant no. 332148), and Chinese Scholarship Council (CSC) grant no. 202306260040.

CRediT authorship contribution statement

Ólafur Eysteinn Sigurjónsson: Validation, Resources, Methodology. **Qianli Ma:** Writing – review & editing, Supervision, Methodology, Investigation, Formal analysis, Data curation, Conceptualization. **Qiang Wang:** Writing – review & editing, Writing – original draft, Visualization, Validation, Methodology, Funding acquisition, Formal analysis, Conceptualization. **Håvard Jostein Haugen:** Writing – review & editing, Supervision, Software, Resources, Project administration, Methodology, Funding acquisition, Conceptualization. **Dirk Linke:** Writing – review & editing, Validation, Supervision, Project administration, Conceptualization. **Ståle Petter Lyngstadaas:** Writing – review & editing, Supervision, Resources, Methodology, Funding acquisition, Conceptualization.

Declaration of Competing Interest

The authors declare the following financial interests/personal relationships which may be considered as potential competing interests: Håvard Jostein Haugen has patent #PeriClean™, product H2O2 + Poloxamer licensed to 17/939,670. Ståle Petter Lyngstadaas has patent #PeriClean™, product H2O2 + Poloxamer licensed to 16/420,819. Corticalis AS owns the IP rights for this product, PeriClean™. S.P.L. and H.J.H are shareholders in Corticalis AS. The other authors do not have any conflict of interest. If there are other authors, they declare that they have no known competing financial interests or personal relationships that could have appeared to influence the work reported in this paper.

Appendix A. Supporting information

Supplementary data associated with this article can be found in the online version at doi:10.1016/j.colsurfb.2025.114727.

Data availability

The raw data required to reproduce these findings can be shared upon request with the corresponding author.

References

[1] AJ Miller, LC Brown, G. Wei, MR Durham, FN Hulet, S. Jeyapalina, et al., Dental implant failures in Utah and US veteran cohorts, Clin. Implant Dent. Relat. Res. 26 (3) (2024) 604–614.

[2] H. Chouirfa, H. Bouloussa, V. Migonney, C. Falentin-Daudré, Review of titanium surface modification techniques and coatings for antibacterial applications, Acta Biomater. 83 (2019) 37–54.

[3] T. Berglundh, G. Armitage, MG Araujo, G. Avila-Ortiz, J. Blanco, PM Camargo, et al., Peri-implant diseases and conditions: consensus report of workgroup 4 of the 2017 World Workshop on the classification of periodontal and peri-implant diseases and conditions, J. Clin. Periodontol. 45 (20) (2018) S286–Ss91.

[4] R. Matthes, K. Duske, TG Kebede, C. Pink, R. Schlüter, T. von Woedtke, et al., Osteoblast growth, after cleaning of biofilm-covered titanium discs with air-polishing and cold plasma, J. Clin. Periodontol. 44 (6) (2017) 672–680.

[5] F. Schwarz, J. Derks, A. Monje, HL. Wang, Peri-implantitis, J. Clin. Periodontol. 45 (20) (2018) S246–Ss66.

[6] MG Grusovin, P. Coulthard, HV Worthington, P. George, M. Esposito, Interventions for replacing missing teeth: maintaining and recovering soft tissue health around dental implants, Cochrane Database Syst. Rev. 2010 (8) (2010) Cd003069.

[7] B. Hussain, JI Grytten, G. Rongen, M. Sanz, HJ. Haugen, Surface topography has less influence on peri-implantitis than patient factors: a comparative clinical study of two dental implant systems, Acs Biomater. Sci. Eng. 10 (7) (2024) 4562–4574.

[8] I. Hart, C. Wells, A. Tsigarida, B. Bezerra, Effectiveness of mechanical and chemical decontamination methods for the treatment of dental implant surfaces affected by peri-implantitis: a systematic review and meta-analysis, Clin. Exp. Dent. Res. 10 (1) (2024) e839.

[9] B. Hussain, HJ Haugen, AM Aass, M. Sanz, GN Antonoglou, P. Bouchard, et al., Peri-implant health and the knowing-doing gap-A digital survey on procedures and therapies, Front. Dent. Med. 2 (2021) 726607.

[10] R. Cosgarea, A. Roccuzzo, K. Jepsen, A. Sculean, S. Jepsen, GE. Salvi, Efficacy of mechanical/physical approaches for implant surface decontamination in non-surgical submarginal instrumentation of peri-implantitis. A systematic review, J. Clin. Periodontol. (2022).

[11] L. Al Ghazal, J. O'Sullivan, N. Claffey, I. Polyzois, Comparison of two different techniques used for the maintenance of peri-implant soft tissue health: a pilot randomized clinical trial, Acta Odontol. Scand. 75 (7) (2017) 542–549.

[12] M. Sanz, B. Noguerol, I. Sanz-Sanchez, CHF Hammerle, H. Schliephake, F. Renouard, et al., European association for osseointegration delphi study on the trends in implant dentistry in Europe for the year 2030, Clin. Oral. Implants Res 30 (5) (2019) 476–486.

[13] L. Chen, Z. Tong, H. Luo, Y. Qu, X. Gu, M. Si, Titanium particles in peri-implantitis: distribution, pathogenesis and prospects, Int. J. Oral. Sci. 15 (1) (2023) 49.

[14] D. Herrera, T. Berglundh, F. Schwarz, I. Chapple, S. Jepsen, A. Sculean, et al., Prevention and treatment of peri-implant diseases-The EFP S3 level clinical practice guideline, J. Clin. Periodontol. 50 (26) (2023) 4–76.

[15] M. Stiesch, J. Grischke, P. Schaefer, LJA. Heitz-Mayfield, Supportive care for the prevention of disease recurrence/progression following peri-implantitis treatment: a systematic review, J. Clin. Periodontol. 50 (26) (2023) 113–134.

[16] CH Alves, KL Russi, NC Rocha, F. Bastos, M. Darrieux, TM Parisotto, et al., Host-microbiome interactions regarding peri-implantitis and dental implant loss, J. Transl. Med. 20 (1) (2022) 425.

[17] B. Hussain, HJ Haugen, AM Aass, M. Sanz, GN Antonoglou, P. Bouchard, et al., Peri-implant health and the knowing-doing gap-a digital survey on procedures and therapies, Front. Dent. Med. 2 (76) (2021).

[18] C. Patil, A. Agrawal, SS Abullais, S. Arora, SU Khateeb, AEM. Fadul, Effectiveness of different chemotherapeutic agents for decontamination of infected dental implant surface: a systematic review, Antibiotics 11 (5) (2022).

[19] P. James, HV Worthington, C. Parnell, M. Harding, T. Lamont, A. Cheung, et al., Chlorhexidine mouthrinse as an adjunctive treatment for gingival health, Cochrane Database Syst. Rev. 3 (3) (2017) Cd008676.

[20] M. Sanz, J. Serrano, M. Iniesta, I. Santa Cruz, D. Herrera, Antiplaque and antigingivitis toothpastes, Monogr. Oral. Sci. 23 (2013) 27–44.

[21] MF Silva, NB dos Santos, B. Stewart, W. DeVizio, HM. Proskin, A clinical investigation of the efficacy of a commercial mouthrinse containing 0.05% cetylpyridinium chloride to control established dental plaque and gingivitis, J. Clin. Dent. 20 (2) (2009) 55–61.

[22] Y. Almoshari, R. Ren, H. Zhang, Z. Jia, X. Wei, N. Chen, et al., GSK3 inhibitor-loaded osteotropic Pluronic hydrogel effectively mitigates periodontal tissue damage associated with experimental periodontitis, Biomaterials 261 (2020) 120293.

[23] VH Chung, AY Chen, LB Jeng, CC Kwan, SH Cheng, SC. Chang, Engineered autologous bone marrow mesenchymal stem cells: alternative to cleft alveolar bone graft surgery, J. Craniofac Surg. 23 (5) (2012) 1558–1563.

[24] P. He, H. Zhang, Y. Li, M. Ren, J. Xiang, Z. Zhang, et al., 1α,25-Dihydroxyvitamin D3-loaded hierarchical titanium scaffold enhanced early osseointegration, Mater. Sci. Eng. C. Mater. Biol. Appl. 109 (2020) 110551.

[25] B. Hussain, S. Khan, AE Agger, JE Ellingsen, SP Lyngstadaas, J. Bueno, et al., A comparative investigation of chemical decontamination methods for in-situ cleaning of dental implant surfaces, J. Funct. Biomater. 14 (8) (2023).

[26] B. Hussain, R. Simm, J. Bueno, S. Giannettou, AO Naemi, SP Lyngstadaas, et al., Biofouling on titanium implants: a novel formulation of poloxamer and peroxide for in situ removal of pellicle and multi-species oral biofilm, Regen. Biomater. 11 (2024) rbae014.

[27] J. Perussolo, N. Donos, Maintenance of peri-implant health in general dental practice, Br. Dent. J. 236 (10) (2024) 781–789.

[28] N. West, I. Chapple, S. Culshaw, N. Donos, I. Needleman, J. Suvan, et al., BSP Implementation of prevention and treatment of peri-implant diseases - The EFP S3 level clinical practice guideline, J. Dent. 149 (2024) 104980.

[29] F. Schwarz, M. Herten, M. Sager, M. Wieland, M. Dard, J. Becker, Histological and immunohistochemical analysis of initial and early osseous integration at chemically modified and conventional SLA titanium implants: preliminary results of a pilot study in dogs, Clin. Oral. Implants Res. 18 (4) (2007) 481–488.

[30] JE. Davies, Mechanisms of endosseous integration, Int. J. Prosthodont. 11 (5) (1998) 391–401.

[31] I. Ericsson, J. Lindhe, Probing depth at implants and teeth. An experimental study in the dog, J. Clin. Periodontol. 20 (9) (1993) 623–627.

[32] T. Guo, K. Gulati, H. Arora, P. Han, B. Fournier, S. Ivanovski, Race to invade: understanding soft tissue integration at the transmucosal region of titanium dental implants, Dent. Mater. 37 (5) (2021) 816–831.

[33] EM Czekanska, MJ Stoddart, JR Ralphs, RG Richards, JS. Hayes, A phenotypic comparison of osteoblast cell lines versus human primary osteoblasts for biomaterials testing, J. Biomed. Mater. Res. A 102 (8) (2014) 2636–2643.

[34] SF Lamolle, M. Monjo, M. Rubert, HJ Haugen, SP Lyngstadaas, JE. Ellingsen, The effect of hydrofluoric acid treatment of titanium surface on nanostructural and chemical changes and the growth of MC3T3-E1 cells, Biomaterials 30 (5) (2009) 736–742.

[35] SL Percival, R. Chen, D. Mayer, AM. Salisbury, Mode of action of poloxamer-based surfactants in wound care and efficacy on biofilms, Int. Wound J. 15 (5) (2018) 749–755.

[36] G. Camana, M. Tavano, M. Li, F. Castiglione, F. Rossi, F. Cellesi, Design of functional pluronic-based precursors for tailoring hydrogel thermoresponsiveness and cell-adhesive properties, Materials 16 (7) (2023).

[37] S. Chen, Y. Guo, R. Liu, S. Wu, J. Fang, B. Huang, et al., Tuning surface properties of bone biomaterials to manipulate osteoblastic cell adhesion and the signaling pathways for the enhancement of early osseointegration, Colloids Surf. B Biointerfaces 164 (2018) 58–69.

[38] X. Shi, M. Nakagawa, G. Kawachi, L. Xu, K. Ishikawa, Surface modification of titanium by hydrothermal treatment in Mg-containing solution and early osteoblast responses, J. Mater. Sci. Mater. Med. 23 (5) (2012) 1281–1290.

[39] K. Katoh, FAK-dependent cell motility and cell elongation, Cells 9 (1) (2020).

[40] JL Bays, KA. DeMali, Vinculin in cell-cell and cell-matrix adhesions, Cell Mol. Life Sci. 74 (16) (2017) 2999–3009.

[41] CX Wang, T. Ma, MY Wang, HZ Guo, XY Ge, Y. Zhang, et al., Facile distribution of an alkaline microenvironment improves human bone marrow mesenchymal stem cell osteogenesis on a titanium surface through the ITG/FAK/ALP pathway, Int. J. Implant Dent. 7 (1) (2021) 56.

[42] PW Kämmerer, AM Pabst, M. Dau, H. Staedt, B. Al-Nawas, M. Heller, Immobilization of BMP-2, BMP-7 and alendronic acid on titanium surfaces: adhesion, proliferation and differentiation of bone marrow-derived stem cells, J. Biomed. Mater. Res. A 108 (2) (2020) 212–220.

[43] SJ Qian, YW Tsai, T. Koutouzis, HC Lai, SC Qiao, GA. Kotsakis, Impact of surface chemical treatment in surgical regenerative treatment of ligature-induced peri-implantitis: a canine study, J. Periodontol. 95 (10) (2024) 991–1001.

[44] F. Chellini, M. Giannelli, A. Tani, L. Ballerini, L. Vallone, D. Nosi, et al., Mesenchymal stromal cell and osteoblast responses to oxidized titanium surfaces pre-treated with $\lambda = 808$ nm GaAlAs diode laser or chlorhexidine: in vitro study, Lasers Med. Sci. 32 (6) (2017) 1309–1320.

[45] S. Balloni, P. Locci, A. Lumare, L. Marinucci, Cytotoxicity of three commercial mouthrinses on extracellular matrix metabolism and human gingival cell behaviour, Toxicol. Vitr. 34 (2016) 88–96.

[46] F. Di Spirito, F. Giordano, MP Di Palo, F. D'Ambrosio, B. Scognamiglio, G. Sangiovanni, et al., Microbiota of peri-implant healthy tissues, peri-implant mucositis, and peri-implantitis: a comprehensive review, Microorganisms 12 (6) (2024).

[47] E. Suszcynsky-Meister, S. St John, E. Schneiderman, In vitro safety evaluation of a hydrogen peroxide whitening emulsion technology on human enamel and dentin, Am. J. Dent. 35 (3) (2022) 115–122.

[48] LJ. Walsh, Safety issues relating to the use of hydrogen peroxide in dentistry, Aust. Dent. J. 45 (4) (2000) 257–269, quiz 89.

[49] AA Fatokun, TW Stone, RA. Smith, Hydrogen peroxide-induced oxidative stress in MC3T3-E1 cells: the effects of glutamate and protection by purines, Bone 39 (3) (2006) 542–551.

[50] T. Chidawanyika, S. Supattapone, Hydrogen peroxide-induced cell death in mammalian cells, J. Cell Signal 2 (3) (2021) 206–211.

[51] X. Deng, D. Jing, H. Liang, D. Zheng, Z. Shao, H_2O_2 damages the stemness of rat bone marrow-derived mesenchymal stem cells: developing a "Stemness Loss" model, Med. Sci. Monit. 25 (2019) 5613–5620.

[52] R. Chihara, H. Kitajima, Y. Ogawa, H. Nakamura, S. Tsutsui, M. Mizutani, et al., Effects of residual H(2)O(2) on the growth of MSCs after decontamination, Regen. Ther. 9 (2018) 111–115.

[53] M. Li, L. Zhao, J. Liu, AL Liu, WS Zeng, SQ Luo, et al., Hydrogen peroxide induces G2 cell cycle arrest and inhibits cell proliferation in osteoblasts, Anat. Rec. (Hoboken) 292 (8) (2009) 1107–1113.

[54] ZS Xu, XY Wang, DM Xiao, LF Hu, M. Lu, ZY Wu, et al., Hydrogen sulfide protects MC3T3-E1 osteoblastic cells against H2O2-induced oxidative damage-implications for the treatment of osteoporosis, Free Radic. Biol. Med. 50 (10) (2011) 1314–1323.

[55] AM Iannuzzi, C. Giacomelli, M. De Leo, D. Pietrobono, F. Camangi, N. De Tommasi, et al., Antioxidant activity of compounds isolated from elaeagnus umbellata promotes human gingival fibroblast well-being, J. Nat. Prod. 83 (3) (2020) 626–637.

[56] X. Han, Z. Wang, X. Wang, X. Zheng, J. Ma, Z. Wu, Microbial responses to membrane cleaning using sodium hypochlorite in membrane bioreactors: cell integrity, key enzymes and intracellular reactive oxygen species, Water Res. 88 (2016) 293–300.
[57] Y. Sun, C. Wang, L. Wen, Z. Ling, J. Xia, B. Cheng, et al., Quercetin ameliorates senescence and promotes osteogenesis of BMSCs by suppressing the repetitive element-triggered RNA sensing pathway, Int. J. Mol. Med. 55 (1) (2025).
[58] N. Cui, CY Dai, X. Mao, X. Lv, Y. Gu, ES Lee, et al., Poloxamer-based scaffolds for tissue engineering applications: a review, Gels 8 (6) (2022).
[59] JH Choi, OK Choi, J. Lee, J. Noh, S. Lee, A. Park, et al., Evaluation of double network hydrogel of poloxamer-heparin/gellan gum for bone marrow stem cells delivery carrier, Colloids Surf. B Biointerfaces 181 (2019) 879–889.
[60] I. Atsuta, Y. Ayukawa, R. Kondo, W. Oshiro, Y. Matsuura, A. Furuhashi, et al., Soft tissue sealing around dental implants based on histological interpretation, J. Prosthodont Res. 60 (1) (2016) 3–11.
[61] AA Al-Khureif, BA Mohamed, AZ Siddiqui, M. Hashem, AA Khan, DD. Divakar, Clinical, host-derived immune biomarkers and microbiological outcomes with adjunctive photochemotherapy compared with local antimicrobial therapy in the treatment of peri-implantitis in cigarette smokers, Photo Photo Ther. 30 (2020) 101684.
[62] I. Fragkioudakis, A. Kallis, E. Kesidou, O. Damianidou, D. Sakellari, I. Vouros, Surgical treatment of peri-implantitis using a combined Nd: YAG and Er: YAG laser approach: investigation of clinical and bone loss biomarkers, Dent. J. 11 (3) (2023).
[63] A. Hagiu, T. Attin, PR Schmidlin, LL. Ramenzoni, Dose-dependent green tea effect on decrease of inflammation in human oral gingival epithelial keratinocytes: in vitro study, Clin. Oral. Invest. 24 (7) (2020) 2375–2383.
[64] M. Yang, H. Liu, Y. Wang, G. Wu, S. Qiu, C. Liu, et al., Hypoxia reduces the osteogenic differentiation of peripheral blood mesenchymal stem cells by upregulating Notch-1 expression, Connect Tissue Res. 60 (6) (2019) 583–596.
[65] Y. Dong, T. Long, C. Wang, AJ Mirando, J. Chen, RJ O'Keefe, et al., NOTCH-mediated maintenance and expansion of human bone marrow stromal/stem cells: a technology designed for orthopedic regenerative medicine, Stem Cells Transl. Med 3 (12) (2014) 1456–1466.
[66] S. Kalomoiris, AC Cicchetto, K. Lakatos, JA Nolta, FA. Fierro, Fibroblast growth factor 2 regulates high mobility group A2 expression in human bone marrow-derived mesenchymal stem cells, J. Cell Biochem. 117 (9) (2016) 2128–2137.
[67] E. Desideri, S. Castelli, C. Dorard, S. Toifl, GL Grazi, MR Ciriolo, et al., Impaired degradation of YAP1 and IL6ST by chaperone-mediated autophagy promotes proliferation and migration of normal and hepatocellular carcinoma cells, Autophagy 19 (1) (2023) 152–162.
[68] V. Damerell, MA Ambele, S. Salisbury, A. Neumann-Mufweba, C. Durandt, MS Pepper, et al., The c-Myc/TBX3 axis promotes cellular transformation of sarcoma-initiating cells, Front. Oncol. 11 (2021) 801691.
[69] RW. Craig, MCL1 provides a window on the role of the BCL2 family in cell proliferation, differentiation and tumorigenesis, Leukemia 16 (4) (2002) 444–454.
[70] H. Zhang, QY He, GC Wang, DK Tong, RK Wang, WB Ding, et al., miR-422a inhibits osteosarcoma proliferation by targeting BCL2L2 and KRAS, Biosci. Rep. 38 (2) (2018).
[71] SK Cho, K. Lee, JH Woo, JH. Choi, Macrophages promote ovarian cancer-mesothelial cell adhesion by upregulation of ITGA2 and VEGFC in mesothelial cells, Cells 12 (3) (2023).
[72] JA Kreidberg, MJ Donovan, SL Goldstein, H. Rennke, K. Shepherd, RC Jones, et al., Alpha 3 beta 1 integrin has a crucial role in kidney and lung organogenesis, Development 122 (11) (1996) 3537–3547.
[73] J. Kim, DW Erikson, RC Burghardt, TE Spencer, G. Wu, KJ Bayless, et al., Secreted phosphoprotein 1 binds integrins to initiate multiple cell signaling pathways, including FRAP1/mTOR, to support attachment and force-generated migration of trophectoderm cells, Matrix Biol. 29 (5) (2010) 369–382.
[74] MF Kunrath, R. Hubler, RM Silva, M. Barros, ER Teixeira, A. Correia, Influence of saliva interaction on surface properties manufactured for rapid osseointegration in dental implants, Biofouling 37 (7) (2021) 757–766.
[75] M. Hirota, T. Ikeda, Y. Sugita, M. Ishijima, S. Hirota, T. Ogawa, Impaired osteoblastic behavior and function on saliva-contaminated titanium and its restoration by UV treatment, Mater. Sci. Eng. C. Mater. Biol. Appl. 100 (2019) 165–177.
[76] A. Pilloni, MA Rojas, L. Marini, P. Russo, Y. Shirakata, A. Sculean, et al., Healing of intrabony defects following regenerative surgery by means of single-flap approach in conjunction with either hyaluronic acid or an enamel matrix derivative: a 24-month randomized controlled clinical trial, Clin. Oral. Invest. 25 (8) (2021) 5095–5107.
[77] Manuel Rodríguez-Aranda II-B, Francisco Alpiste-Illueca, Andrés López-Roldán, Hyaluronic acid for periodontal tissue regeneration in intrabony defects. A systematic review, Andrés, Dent. Rev. 2 (3) (2022).
[78] A. De Lauretis, Ø Øvrebø, M. Romandini, SP Lyngstadaas, F. Rossi, HJ. Haugen, From basic science to clinical practice: a review of current periodontal/mucogingival regenerative biomaterials, Adv. Sci. 11 (17) (2024) e2308848.